

Polarization Dependence of L - and M -Edge Resonant Inelastic X-ray Scattering on Transition-Metal Compounds

Michel van Veenendaal
*Dept. of Physics, Northern Illinois University,
 De Kalb, Illinois 60115 and
 Advanced Photon Source, Argonne National Laboratory,
 9700 South Cass Avenue, Argonne, Illinois 60439*

(Dated: December 19, 2005)

The Resonant Inelastic X-ray Scattering (RIXS) cross section at the L and M edges of transition-metal compounds is studied using an effective scattering operator. The intensities of the elastic peak and for spin-flip processes are derived. A detailed analysis of the polarization and angular dependence of L - and M -edge RIXS for divalent copper compounds, such as the high- T_c superconductors, is given.

PACS numbers: 78.70.Ck, 71.27.+a, 61.10.Dp

Recently, Resonant Inelastic X-ray Scattering (RIXS) at the transition-metal L and M edges has attracted considerable attention [1–4]. In this technique, the incoming X-ray with energy $\hbar\omega$ excites an electron from the $2p$ (L edge) or $3p$ (M edge) core level into the $3d$ valence shell. The energy $\hbar\omega'$ of the outgoing X-ray resulting from the radiative transition from the valence shell to the core level is measured. Since the final state does not contain a core hole, the energy lost by the scattered photon is directly related to excitations created in the valence shell. The use of a particular resonance makes RIXS chemically selective. Combined with the bulk sensitivity, RIXS can provide insight into the electronic and magnetic properties of, for example, complex and nanostructured materials that might be inaccessible with non-resonant techniques. Recently, this technique has been used to study dd transitions in high- T_c superconductors and related materials [1, 2], and spin flips in NiO [3]. Although the spectral line shape of RIXS at the transition-metal L and M edges can often be calculated with numerical methods [4], the analytical understanding of this spectroscopy is still limited. In this Letter, we use an effective scattering operator approach to gain insight into the strength of transitions, such as the elastic peak and spin-flip processes and demonstrate how to use the polarization and angular dependence to selectively probe particular final states.

RIXS is generally well described by the Kramers-Heisenberg equation [4]

$$I(\omega, \omega') = \sum_f |A_f(\omega)|^2 \delta(\hbar\omega + E_g - \hbar\omega' - E_f),$$

where we denote ground and final states by g and f , respectively. For dipolar transitions, the scattering amplitude is given by $A_f(\omega) = \langle f | \mathbf{e}'^* \cdot \mathbf{r} G(\omega) \mathbf{e} \cdot \mathbf{r} | g \rangle$, where \mathbf{e} and \mathbf{e}' are the polarization vectors of the incoming and outgoing photon, respectively. The intermediate state Green's function is given by $G(\omega) = \sum_n (\hbar\omega - E_n + i\Gamma/2)^{-1}$ with E_n the intermediate-state energies and Γ the broadening due to the finite lifetime of the core hole.

In order to write the scattering amplitude in terms of an effective dd operator, Luo, Hannon, and Trammell [5] applied a fast-collision approximation to the intermediate-state propagator. In their derivation, they included the fact that the absorption spectrum is split into two distinct peaks due to the large core-hole spin-orbit coupling. Within this approximation, the Green function can be written as $\overline{G}^\pm(\omega) = (\hbar\omega - \overline{E}_{j^\pm} + i\Gamma/2)^{-1}$, where \overline{E}_{j^\pm} is the mean energy for a spin-orbit split edge with $j^\pm = \frac{3}{2}, \frac{1}{2}$ for transition-metal ions. Using spherical tensor analysis, Luo *et al.* [5] were able to derive the scattering amplitude for a particular absorption edge j^\pm

$$A_f^\pm(\omega) = P_{2p3d}^2 \sum_{Q=0}^2 \sum_{q=-Q}^Q \overline{G}^\pm(\omega) T_{Qq}^*(\mathbf{e}, \mathbf{e}') \langle f | W_{Qq}^\pm | g \rangle,$$

where P_{2p3d} is the reduced matrix element between the $2p$ core level and the $3d$ valence shell. This result describes the RIXS as an effective dd transition made by the operator W_{Qq}^\pm weighted by the polarization dependence $T_{Qq}(\mathbf{e}, \mathbf{e}') = 3(-1)^{1+Q} \sum_{q_1 q_2} e'_{q_2} e_{q_1} C_{1q_1, 1q_2}^{Qq} C_{11, 11}^{Q0}$ where $C_{lm, l'm'}^{Qq}$ is a Clebsch-Gordan coefficient. W_{Qq}^\pm is a one-particle tensor operator of rank Q . The values of $Q = 0, 1, 2$ follow from the combination of the two dipolar transitions, which are tensors of rank 1. The components of the operator are $q = -Q, \dots, Q$. The operator can be expressed as $W_{Qq}^\pm = \sum_{m, s_z, \Delta m, \Delta s_z} a_{Qq}^\pm(m, s_z, \Delta m, \Delta s_z) d_{m+\Delta m, s_z+\Delta s_z}^\dagger d_{ms_z}^\dagger$, where $q = \Delta m + \Delta s_z$, a_{Qq}^\pm is a coefficient that depends on the value of j^\pm , and $d_{ms_z}^\dagger$ creates an electron in the $3d$ orbital with orbital moment $m = 0, \pm 1, \pm 2$ and spin $s_z = \pm \frac{1}{2} = \uparrow, \downarrow$. The W_{Qq}^\pm operate on holes since the absorption process first places an electron in the valence shell ($2p \rightarrow 3d$) and the subsequent deexcitation ($3d \rightarrow 2p$) removes an electron. The scattering operator is expressed as a combination of orbital- and spin-dependent tensor operators of rank Q [5, 6], such as, the number of holes \underline{n} the spin-orbit coupling $\mathbf{L} \cdot \mathbf{S}$ ($Q = 0$), the orbital moment \mathbf{L} , and the spin \mathbf{S} ($Q = 1$).

The result of Luo, Hannon, and Trammell [5] has been used in resonant X-ray scattering (RXS) where $|f\rangle = |g\rangle$. In this case, no angular momentum is transferred to the system, and only the $q = \Delta m + \Delta s_z = 0$ components of the scattering operators contribute to the intensity. For RXS, the intensities of the Bragg peaks are proportional to the ground-state expectation value of an operator, $\langle g|W_{Q0}^\pm|g\rangle$. However, apart from establishing that the operators are nonzero, often there is no need to calculate the expectation value of the operators. In RIXS, on the other hand, the W_{Qq}^\pm cause the scattering of holes, and it is useful to establish how the intensities of the final states depend on the polarization geometry. To find these, we need to know what transitions are made by the operators W_{Qq}^\pm in point-group symmetries relevant for transition-metal compounds.

Let us first discuss the scattering operators in a qualitative way, before giving detailed expression of the W_{Qq}^\pm . The operator W_{Qq}^\pm transfers a total angular momentum $q = \Delta m + \Delta s_z$ to the solid, which can be used to change the orbital moment by Δm or the spin by Δs_z . We can distinguish the following situations: the spin is unchanged, giving $\Delta s_z = 0$ and $\Delta m = q$, or a spin is flipped where $\Delta s_z = \pm 1$ and $\Delta m = q \mp 1$. The possibilities for different q values are summarized in Fig. 1(a). Note that $|q| \leq Q$ and $Q = 0, 1, 2$. To understand the RIXS in transition-metal compounds, we prefer a basis set that better reflects the lower local symmetries resulting from solid-state effects. The effect of the scattering operator is best understood within a basis that is close to the atomic orbitals. This also leads to the simplest expressions for the scattering operators with real coefficients. To obtain eigenstates of the crystal field in point-group symmetries common for transition-metal compounds, such as O_h , D_{4h} and T_d , we combine the $m = \pm 2$ components, $d_{2^\pm s_z}^\dagger = \frac{1}{\sqrt{2}}(d_{2s_z}^\dagger \pm d_{-2s_z}^\dagger)$. Note that the atomic orbitals with $m = \pm 1$ are degenerate in these symmetries. The creation operator in the new basis set is now $d_{\alpha s_z}^\dagger$ with $\alpha = 0, \pm 1, 2^\pm$. The index α denotes an atomic orbital for $\alpha = 0, \pm 1$ and a linear combination of atomic orbitals for $\alpha = 2^\pm$. The new orbitals are related to the real 3d orbitals, $d_{0s_z}^\dagger = d_{3z^2-r^2, s_z}^\dagger$, $d_{2^+ s_z}^\dagger = d_{x^2-y^2, s_z}^\dagger$, $d_{2^- s_z}^\dagger = id_{xy, s_z}^\dagger$, and $d_{\pm 1, s_z}^\dagger = \frac{1}{\sqrt{2}}(-id_{yz, s_z}^\dagger \pm d_{zx, s_z}^\dagger)$. Typical energy splittings due to a crystal field are given in Fig. 1(b).

Figure 1(d) shows how this lower-symmetry basis set can be related to the scattering process. The situation is equivalent to atomic orbitals except when the 2^\pm orbitals are involved. As an example, let us take the situation where $\alpha = 1$, and the scattering operator increases the orbital moment by $\Delta m = 1$, see Fig. 1(d). The hole is then scattered into the atomic orbital with $m = 2$. However, this is not an eigenstate of the crystal field and, since $d_{2s_z}^\dagger = \frac{1}{\sqrt{2}}(d_{2^+ s_z}^\dagger + d_{2^- s_z}^\dagger)$, the hole scatters with equal probability into the 2^+ ($x^2 - y^2$) and 2^- (xy) orbitals. Let us now consider another example where we add $\Delta m = 1$ to the 2^\pm orbitals. The 2^\pm orbitals are a

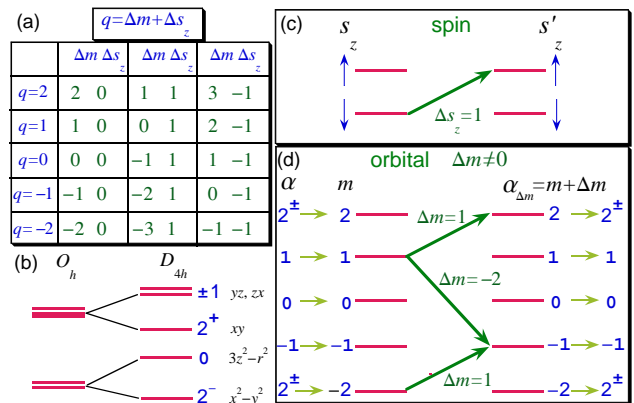


FIG. 1: (color online) (a) Changes in Δm and Δs_z that can be made for a total angular momentum $q = \Delta m + \Delta s_z$. (b) Typical energy splittings of one hole in a 3d orbital in the presence of a crystal field in O_h and D_{4h} symmetry. (c),(d) The effective transition operator W_{Qq}^\pm scatters holes from a state with orbital index α and spin s_z to a state with index $\alpha_{\Delta m}$ and spin $s_z + \Delta s_z$. To obtain the corresponding index $\alpha_{\Delta m}$, we first determine what atomic orbitals are contained in α . Note that $\alpha = 0, \pm 1$ are atomic orbitals with $m = 0, \pm 1$ and that $\alpha = 2^\pm$ is a linear combination of atomic orbitals with $m = \pm 2$. Addition of Δm changes the orbital moment of the hole from m to $m + \Delta m$. Therefore, the final state indices always correspond to atomic orbitals, i.e., $\alpha_{\Delta m} = m + \Delta m$. Note, however, that if $\alpha_{\Delta m} = \pm 2$, the hole ends up in the 2^\pm orbitals since $d_{\pm 2, s_z}^\dagger = \frac{1}{\sqrt{2}}(d_{2^+ s_z}^\dagger \pm d_{2^- s_z}^\dagger)$. Note this schedule only applies to $\Delta m \neq 0$.

linear combination of the atomic orbitals with $m = \pm 2$. Addition of $\Delta m = 1$ to the $m = 2$ is not possible. Addition of $\Delta m = 1$ to $m = -2$ leads to scattering of the hole into an atomic orbital with $m = -1$. Therefore, for $\Delta m = 1$ a hole in the $x^2 - y^2$ orbital or xy orbital scatters with equal probability into the yz and zx orbitals. For $\Delta m = 0$, we do not expect orbital scattering for atomic orbitals. However, within crystal-field symmetries, transitions can be made for the 2^\pm orbitals. If the orbital part of a tensor operator has an odd rank, holes in the 2^\pm orbital scatter into 2^\mp orbitals. The indices are $\alpha_0 = 0, \pm 1, 2^\mp$ for $\alpha = 0, \pm 1, 2^\pm$. If the orbital part of a tensor operator has an even rank, no scattering occurs.

The power in this approach is to understand how one can selectively probe the different scattering operators W_{Qq}^\pm using the polarization dependence T_{Qq} . For $Q = 0$, the polarization dependence is given by $T_{00} = \mathbf{e}^* \cdot \mathbf{e}$ and the scattering operator is

$$W_{00}^\pm = \sum_{\alpha s_z} \left\{ \left(j^\pm + \frac{1}{2} \right) n_{\alpha s_z} \pm \mu s_z d_{\alpha_0 s_z} d_{\alpha s_z}^\dagger \right\} \pm \sqrt{2} \sum_{\alpha} (a_{\alpha}^1 d_{\alpha_1 \downarrow} d_{\alpha \uparrow}^\dagger - a_{\alpha}^{-1} d_{\alpha_{-1} \uparrow} d_{\alpha \downarrow}^\dagger), \quad (1)$$

where $\mu = 0, \pm 1, 2$ for $\alpha = 0, \pm 1, 2^\pm$. The coefficients a_{α}^q result from factors due to the step-up and step-down operators and the normalization of the wavefunc-

tions and are $a_{\alpha}^{\pm 1} = \pm \frac{\sqrt{3}}{2}, \pm \frac{1}{2}, -\frac{1}{2}$ for $\alpha = 0, 2^+, 2^-$, $a_1^1 = a_{-1}^{-1} = \frac{1}{\sqrt{2}}$, and $a_{\mp 1}^{\pm 1} = \pm \frac{\sqrt{3}}{2}$. From the first term on the right-hand side, it is clear that W_{00}^{\pm} will always give elastic scattering with an intensity proportional to the number of holes in the ground state squared $(j^{\pm} + \frac{1}{2})^2 |\langle g | \sum_{\alpha s_z} n_{\alpha s_z} | g \rangle|^2$. Note that the intensity is weaker at the j^- edge compared to the j^+ edge. This elastic contribution is often eliminated by choosing the polarizations such that $\mathbf{e}'^* \cdot \mathbf{e} = 0$. For example, for a 90° scattering angle with \mathbf{e} in the scattering plane [$\varphi = 0$, see Fig. 2(a)], the incoming polarization vector \mathbf{e} is perpendicular to both outgoing polarization vectors \mathbf{e}'_1 and \mathbf{e}'_2 . By turning \mathbf{e} out of the scattering plane, T_{00} becomes non zero and an elastic peak appears. This is particularly dominant for early transition-metal compounds as was demonstrated for TiO_2 by Harada *et al.* [7]. However, W_{10}^{\pm} and W_{20}^{\pm} also contribute to the elastic line. For example,

$$W_{10}^{\pm} = \sum_{\alpha s_z} \left\{ -\left(j^{\pm} + \frac{1}{2}\right) \frac{\mu}{2} d_{\alpha_0 s_z} d_{\alpha s_z}^{\dagger} \mp \frac{2}{3} (\mu^2 - 1) s_z n_{\alpha s_z} \right\} \\ \mp \frac{\sqrt{2}}{3} \sum_{\alpha} \left\{ (2\mu_1 + 1) a_{\alpha}^1 d_{\alpha_{1\downarrow}} d_{\alpha\uparrow}^{\dagger} - (2\mu_{-1} - 1) a_{\alpha}^{-1} d_{\alpha_{-1\uparrow}} d_{\alpha\downarrow}^{\dagger} \right\}, \quad \mp \sum_{\alpha} \left\{ \frac{q\sqrt{2}}{6} (\mu^2 - 4) d_{\alpha, \frac{q}{2}} d_{\alpha, -\frac{q}{2}}^{\dagger} - \frac{2q}{\sqrt{3}} a_{\alpha}^{2q} d_{\alpha_{2q, -\frac{q}{2}}} d_{\alpha, \frac{q}{2}}^{\dagger} \right\}$$

where $\mu_q = (-q)^{\mu-1} \mu$. The intensity of the elastic peak arising from the second term on the right-hand side is $\frac{1}{9} |\langle g | (2Q_z + 1) S_z | g \rangle|^2$, where $Q_z = \mu^2 - 2$ is the quadrupolar moment. This is usually significantly smaller than the intensity $(j^{\pm} + \frac{1}{2})^2 |\langle g | n_h | g \rangle|^2$ due to the W_{00}^{\pm} term. In particular, it is zero for TiO_2 , since $S_z = 0$ for the $3d^0$ ground state, consistent with experiments [7].

In more complex systems, a local $\alpha s_z \rightarrow \alpha s_z$ transition is not necessarily elastic due to band effects. In the literature, there has been controversy whether the RIXS data on the ladder compound NaV_2O_5 should be ascribed to a transition between the bonding and antibonding states of the xy orbital of the two vanadium atoms on a rung of the ladder or to a local $xy \rightarrow yz/zx$ crystal-field transition [8]. In the 90° scattering geometry that was used experimentally [8], the transitions $xy \rightarrow xy$ are strongly suppressed since the W_{00}^{\pm} scattering operator does not contribute to the RIXS cross section. Using the expressions for the scattering operators, it can be shown that, at the L_3 edge, the intensity of the $xy \rightarrow yz/zx$ transition is about six times larger than the $xy \rightarrow xy$ transition. In addition, the presence of a strong xy bonding-antibonding transition should be accompanied by the presence of a strong elastic peak, which results from the same $xy \rightarrow xy$ scattering process. However, this is not observed experimentally [8].

De Groot, Kuiper, and Sawatzky [9] demonstrated numerically that spin-flip processes ($\Delta s_z = \pm 1$), that are not accessible with low-energy optical spectroscopy, can be obtained with RIXS. Let us first consider the situation where the orbital does not change, i.e., $\Delta m = 0$. This can be achieved by the step operators for the spin $S_{\pm 1}$,

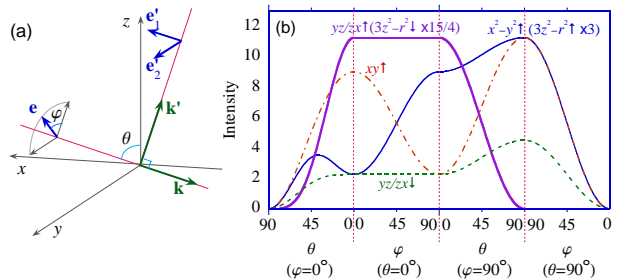


FIG. 2: (color online) (a) A typical 90° scattering geometry. (b) RIXS intensities as a function of the angle θ of the incoming radiation with the surface normal and the angle φ of the incoming polarization vector with the scattering plane for a ground state of a hole in the $x^2 - y^2 \uparrow$ orbital.

which are contained in $W_{1,\pm 1}^{\pm}$. For $q = \pm 1$, we have

where $a_{\alpha}^{\pm 2} = \pm \frac{1}{\sqrt{2}}, \frac{1}{\sqrt{2}}, \mp \frac{1}{\sqrt{2}}$ for $\alpha = 0, 2^+, 2^-$, $a_1^2 = a_{-1}^{-2} = 0$, and $a_{-1}^{-2} = a_1^{-2} = \sqrt{\frac{3}{2}}$. The polarization dependence for these operators is given by $T_{1q}(\mathbf{e}, \mathbf{e}') = -\frac{3}{2} i (\mathbf{e}'^* \times \mathbf{e})_q$. The second term on the right-hand side is a spin flip process. The coefficient $\frac{q\sqrt{2}}{6} (\mu^2 - 4)$ shows that spin-flip processes for holes in the $x^2 - y^2$ and xy orbitals ($\mu = 2$) are prohibited. This directly shows why, in numerical calculations for a Cu^{2+} ion [9], spin flips are absent in D_{4h} symmetry where the ground state has a hole in the $x^2 - y^2$ orbital, but are present in O_h symmetry where there is also hole density in the $3z^2 - r^2$ ($\mu = 0$) orbital. Also in NiO , which has two holes in the $x^2 - y^2 \uparrow$ and $3z^2 - r^2 \uparrow$ orbitals, a spin-flip is expected for the hole in the $3z^2 - r^2$ orbital only. In recent RIXS measurements at the M threshold by Chiuzbăian *et al.* [3], this spin-flip feature overlapped with the elastic Rayleigh peak. They therefore considered spin flips in combination with a crystal field transition. These processes occur in both W_{00}^{\pm} and W_{10}^{\pm} . However, in the 90° scattering geometry used, the contribution from W_{00}^{\pm} is zero. The terms in W_{10}^{\pm} giving this scattering are $\frac{1}{\sqrt{6}} d_{1\downarrow} d_{0\uparrow}^{\dagger} + \frac{1}{\sqrt{2}} d_{-1\downarrow} d_{2\uparrow}^{\dagger}$. Note that the spin flip intensity arising from the $\alpha = 2^+$ ($x^2 - y^2$) is larger than that of the $\alpha = 0$ ($3z^2 - r^2$).

Significant work using RIXS at the L and M thresholds has been done on high- T_c superconductors and related compounds [1, 2]. Let us consider the typical experimental situation with linearly polarized incoming X-rays and no polarization analysis of the outgoing x-rays. We take a 90° scattering angle, see Fig. 2(a). The incoming polarization vector is $\mathbf{e} = \cos \varphi (-\cos \theta \mathbf{x} + \sin \theta \mathbf{z}) + \sin \varphi \mathbf{y}$, where \mathbf{x}, \mathbf{y} , and \mathbf{z} are the Cartesian unit vectors with \mathbf{y}

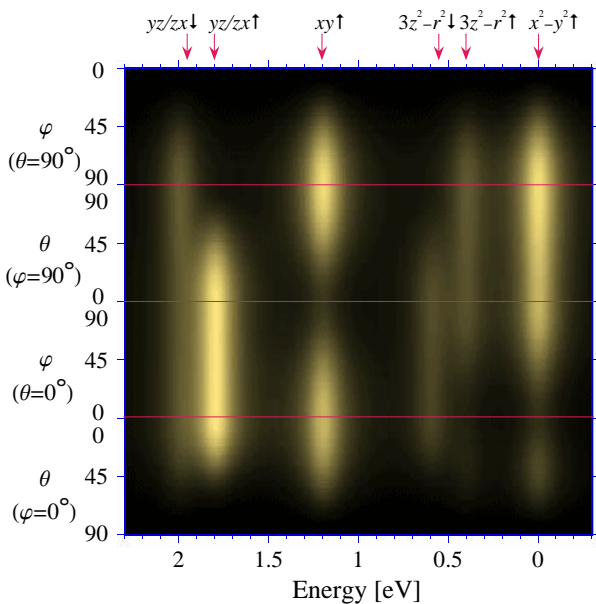


FIG. 3: (color online) Density plot of the RIXS intensities at the L_3 edge for a 90° scattering geometry, see Fig. 2(a), as a function of the angle θ of the incoming radiation with the surface normal and the angle φ between \mathbf{e} and the scattering plane. The ground state has a hole in the $x^2 - y^2 \uparrow$ orbital. The intensities for scattering into $x^2 - y^2 \downarrow$ and $xy \downarrow$ are zero.

perpendicular to the scattering plane; θ is the angle of the incoming x-ray with the surface normal and φ is the angle of the polarization vector with the scattering plane, see Fig. 2(a). The outgoing polarization vectors are then $\mathbf{e}'_1 = \sin \theta \mathbf{x} + \cos \theta \mathbf{z}$ and $\mathbf{e}'_2 = \mathbf{y}$. We take a ground state of a hole in the $x^2 - y^2 \uparrow$ orbital, which gives a good idea of the dd transitions observed in Cu L - and M -edge RIXS. The angular dependence for final states with a hole in the αs_z orbital follows from $\sum_{Qq} (-1)^q \langle \alpha s_z | T_{Qq}^* W_{Qq}^\pm | 2^+ \uparrow \rangle$. It is straightforward to obtain the T_{Qq} from the definition. Using the exact expressions for W_{Qq}^\pm , one finds two distinct angular dependencies:

$$\begin{aligned} f(\theta, \varphi) &= (a \sin 2\theta + b \cos^2 \theta) \cos^2 \varphi + (c \sin \theta + d) \sin^2 \varphi \\ g(\theta, \varphi) &= a(\cos^4 \theta \cos^2 \varphi + \cos^2 \theta \sin^2 \varphi). \end{aligned} \quad (2)$$

The function $f(\theta, \varphi)$ gives the intensities to scatter the hole into $x^2 - y^2 \uparrow$, $3z^2 - r^2 \uparrow$, $xy \uparrow$, and $yz/zx \downarrow$ with coefficients $a, b, c, d = \frac{9}{4}, \frac{9}{4}, \frac{9}{4}, 9; \frac{3}{4}, \frac{3}{4}, \frac{3}{4}, 3; \frac{9}{16}, 9, 9, \frac{9}{4}$ and

$\frac{9}{16}, \frac{9}{4}, \frac{9}{4}, \frac{9}{4}$, respectively. The angular dependencies of the intensities to scatter into $3z^2 - r^2 \downarrow$ and $yz/zx \uparrow$ are given by $g(\theta, \varphi)$ with coefficients 3 and $\frac{45}{4}$, respectively, see Fig. 2(b). The intensities of reaching $x^2 - y^2 \downarrow$ and $xy \downarrow$ are zero. Figure 3 shows a density plot of the intensities at the L_3 or M_3 edge as a function of θ and φ , where the orbital energies with respect to $x^2 - y^2$ are $E_{3z^2-r^2} = 0.4$ eV, $E_{xy} = 1.2$ eV, and $E_{yz/zx} = 1.8$ eV. These are typical crystal field splittings [2], where overlap has been avoided for clarity. We take the energy needed to flip a spin 0.15 eV. As is clear from Fig. 3, employing the strong angular and polarization dependence allows a better identification of the spectral features. First, the intensity for transitions with a spin flip is generally lower than for those without because that transitions without spin flip are preceded by the coefficient $(j^+ + \frac{1}{2})^2 = 4$, which is generally larger than the coefficients determining the spin-flip processes. Also, as expected, we do not find a spin-flip process for the $x^2 - y^2$ orbitals. However, also no transition is found to the $xy \downarrow$ state. This transition would result from the $W_{2,-1}^\pm$ operator, but the spin-flip is preceded by the coefficient $\frac{1}{\sqrt{6}}\mu(\mu^2 - 4)$ and is therefore zero. The intensities are zero for $\theta = 90^\circ$ and $\varphi = 0$, because the absorption is zero for these angles. When turning the polarization vector out of the scattering plane $\varphi = 0 \rightarrow 90^\circ$, we find a strong increase in the elastic peak. Note, however, that taking $\mathbf{e} \cdot \mathbf{e}' = 0$ ($\varphi = 0$) does not reduce the elastic peak entirely to zero, due to the contributions from W_{10}^\pm and W_{20}^\pm .

In conclusion, it has been demonstrated how the use of an effective scattering operator can strongly enhance our understanding of the angle and polarization dependence of the resonant inelastic x-ray scattering cross section. Analytical expressions have been derived that determine the conditions for spin-flip processes and the intensity of the elastic scattering in the RIXS cross section.

We acknowledge useful discussions with Ken Ahn and Serkan Erdin. This work was supported by the U.S. Department of Energy (DE-FG02-03ER46097) and the Institute for Nanoscience, Engineering, and Technology at Northern Illinois University under a grant from the U.S. Department of Education. Work at Argonne National Laboratory was supported by the U.S. Department of Energy, Office of Basic Energy Sciences, under contract W-31-109-ENG-38.

- [1] P. Kuiper *et al.*, Phys. Rev. Lett. **80**, 5204 (1998).
 [2] G. Ghiringhelli *et al.*, Phys. Rev. Lett. **92**, 117406 (2004).
 [3] S. G. Chiuabăian *et al.*, Phys. Rev. Lett. **95**, 197402 (2005).
 [4] For a review, see A. Kotani and S. Shin, Rev. Mod. Phys. **73**, 203 (2001).
 [5] J. Luo, G. T. Trammell, and J. P. Hannon, Phys. Rev.

- Lett. **71**, 287 (1993).
 [6] B. R. Judd, *Second Quantization in Atomic Spectroscopy* (Johns Hopkins University Press, Baltimore, 1967).
 [7] Y. Harada *et al.*, Phys. Rev. B **61**, 12854 (2000).
 [8] G. P. Zhang *et al.*, Phys. Rev. Lett. **88**, 077401 (2002); M. van Veenendaal and A. J. Fedro, *ibid.* **92**, 219701 (2004); L.-C. Duda *et al.*, *ibid.* **93**, 169701 (2004).

- [9] F. M. F. de Groot, P. Kuiper, and G. A. Sawatzky, Phys. Rev. B **57**, 14584 (1998).